JOURNAL OF Materials CHEMISTRY

Effects of nitro substituents on the properties of a ferroelectric liquid crystalline side chain polysiloxane

Magnus Svensson,[a] Bertil Helgee,*[a] Kent Skarp[b] and Gunnar Andersson[b]

[a]*Department of Polymer Technology, Chalmers University of Technology, S-412 96 Göteborg, Sweden*

[b]*Department of Physics, Chalmers University of Technology, S-412 96 Göteborg, Sweden*

The syntheses of chiral liquid crystalline side chain polysiloxanes with lateral nitro substituents in the mesogenic core are described. The influence of the substituents and substituent positions on phase behaviour and electro-optical properties are investigated and compared. The lateral nitro groups strongly affect the phase behaviour of the side chain precursors as well as the liquid crystalline polymers. Properties in smectic A and C* phases are discussed with respect to substituent position. One side chain precursor exhibits very large spontaneous polarization of ~ 700 nC cm^{-2}.

The possibility of designing and using chiral liquid crystalline side chain polymers for technical applications in the future depends on the understanding of structure–property relationships. A vast number of new molecules, architectures and concepts of chiral liquid crystalline side chain polymers have been synthesized, examined and reported[1,2] since the first ferroelectric liquid crystalline polymer was prepared by Shibaev *et al.*[3] in 1984. Research on the effects of structural changes in the different parts of the mesogens like the chiral centre,[4,5] mesogenic core[6–8] and alkyl chain[9–11] has been carried out. The influence of the polymer main-chain on properties has also been investigated.[12–17] Nevertheless, a large part of today's information on structure–property relationships in chiral liquid crystalline polymers relies on extrapolations from research on low molar mass liquid crystals performed during the 1970s.

Concerning lateral substituents Osman[18] has shown that steric effects and thereby the van der Waals volume of the substituent are usually more important with respect to phase behaviour than dipolar interactions. The more detailed influences of lateral substituents depend on the structure of the rigid core and the position of the substituent. Generalizations are difficult, since the effects differ between polar and non-polar mesogens and probably also change from low molar mass to polymer liquid crystals. Using electron attracting substituents Masuda *et al.*[19] showed that substituents in the centre of the mesogenic core not only increased the intermolecular distance, thus destabilizing the liquid crystal behaviour, but also hindered the formation of smectic phases. With multiple substituents where the second and/or third does not increase the steric effect but adds possibilities for polar interactions the smectic phases can be regained.[20] A study by Hird *et al.*[21] shows the same tendencies.

The nitro group with its large dipole moment and electron attracting power offers a way to drastically change the electron distribution in the aromatic core. This has been used to enhance NLO-effects such as second harmonic generation (SHG) in liquid crystals and in liquid crystalline polymers.[22,23]

In the present paper we have studied the effect of introducing a nitro substituent at various aromatic positions in a 4′-alkoxybiphenyl-4-carboxylic acid phenyl ester mesogen. The nitro group was chosen to increase the spontaneous polarization in the chiral smectic C phase. We were particularly interested in how a strong dipole at different locations in the polarizable aromatic core would change phase behaviour and electro-optical properties of a ferroelectric liquid crystalline polymer[24] having a very broad smectic C* phase and good alignment properties. The chiral group is a substituted lactic acid moiety. The nitro group is introduced at the 2- and 3-position in the phenyl ester and at the 3′-position in the biphenyl part. The side-chain precursors are attached to a poly(dimethyl-co-methylhydrogen)siloxane backbone. It was found that the introduction of substituents changes the phase behaviour dramatically depending on position. One of the side-chain precursors only exhibits a 10 °C temperature interval of the N*-phase but in the corresponding polymer smectic phases over a temperature range of 70 °C are again obtained. Another side-chain precursor shows very large spontaneous polarization (nearly 700 nC cm^{-2}).[25,26] The same system shows interesting NLO-properties reported earlier,[27] where a controllable SHG-intensity in the smectic A phase was described for the first time. For the reference system (without nitro substituent), both the low molar mass mesogen and the polymeric liquid crystal have been described in detail previously.[24,28]

Experimental

Techniques

300 MHz ^{1}H NMR spectra were obtained using a Varian VXR300 spectrometer. All spectra were run in $CDCl_3$ or [$^2H_6$] DMSO solutions. Infrared spectra were recorded on a Perkin-Elmer 2000 FT-IR spectrophotometer using KBr pellets. The phase behaviour of the different materials was identified by combining optical microscopy, differential scanning calorimetry and electro-optical measurements. Optical microscopy was performed using a Mettler FP82HT hot stage, Mettler FP80HT central processor and an Olympus BH-2 polarizing microscope. DSC measurements were recorded on a Perkin-Elmer DSC 7 differential scanning calorimeter.

Materials

Materials and reagents were of commercial grade quality and used without further purification unless otherwise noted. Dry toluene and methylene chloride were obtained by passing the solvents through a bed of aluminium oxide (ICN Alumina N-Super I). (+)-2-(4-Hydroxyphenoxy)propionic acid was generously provided by BASF. Poly(dimethylsiloxane-co-methylhydrosiloxane) with a copolymer ratio 2.7/1 and a degree of polymerization of *ca.* 30 (according to manufacturer) and the hydrosilylation catalyst dicyclopentadienylplatinum(II) dichloride were obtained from Wacker Chemie. Size-exclusion chromatography (SEC) analysis in chloroform of the copolymer performed at 30 °C on a Waters WISP712 instrument

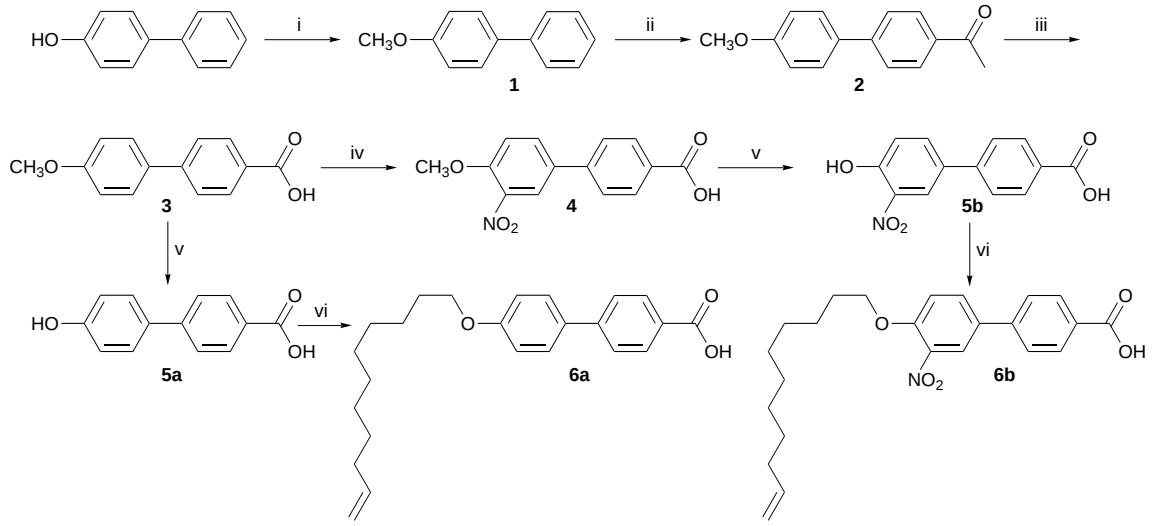

Scheme 1 *Reagents*: i, MeI, KOH, DMF; ii, AcCl, $AlCl_3$, CH_2Cl_2; iii, Br_2, KOH, 1,4-dioxane; iv, HNO_3, AcOH; v, HBr, AcOH; vi, undecenyl bromide, KI, EtOH

equipped with three commercial Styragel columns and Waters 410 refractive index detector gave $\bar{M}_n = 2.6 \cdot 10^3$ g mol^{-1} and $\bar{M}_w = 5.4 \cdot 10^3$ g mol^{-1} with reference to polystyrene standards.

Synthesis

The synthesis of polymers **14a–d** was carried out according to the reactions in Schemes 1–4. All structures were verified by ^{1}H NMR spectroscopy and NMR data were in accordance with the structures in all cases.

4′-Hydroxybiphenyl-4-carboxylic acid 5a. The acid was synthesized from 4-hydroxybiphenyl *via* 4-methoxybiphenyl **1**, 4-acetyl-4′-methoxybiphenyl **2** and 4′-methoxybiphenyl-4-carboxylic acid **3** following closely the procedure reported by Percec *et al.*[29]

4′-Methoxy-3′-nitrobiphenyl-4-carboxylic acid 4. 4′-Methoxybiphenyl-4-carboxylic acid **3** (0.01 mol, 2.28 g) in acetic acid (50 ml) was refluxed with concentrated nitric acid (6 ml) for 15 min. The reaction mixture was poured into water and the precipitate was filtered off. The product recrystallized from ethanol to yield 2.2 g (80%). δ_H ([$^2H_6$] DMSO) 3.98 (s, 3 H), 7.48 (d, 1 H), 7.85 (d, 2 H), 8.02 (d, 2 H), 8.07 (dd, 1 H), 8.26 (d, 1 H).

4′-Hydroxy-3′-nitrobiphenyl-4-carboxylic acid 5b. The acid **5b** was synthesized as for **5a** starting from **4**. δ_H ([$^2H_6$] DMSO)

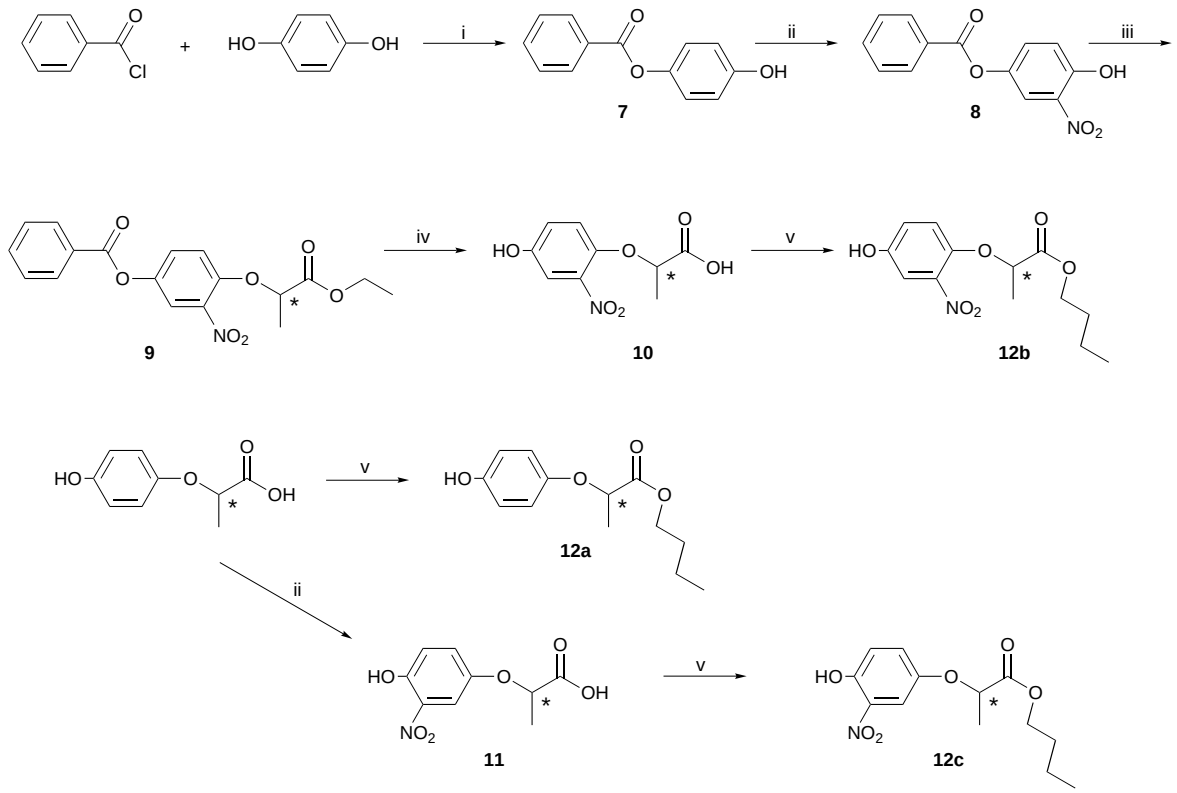

Scheme 2 *Reagents*: i, pyridine, CH_2Cl_2, N_2; ii, HNO_3, AcOH, $<35\,^{\circ}C$; iii, (*S*)-ethyl lactate, PPh_3, diethyl azodicarboxylate, THF, N_2; iv, aq. KOH, EtOH; v, BuOH, HCl(g)

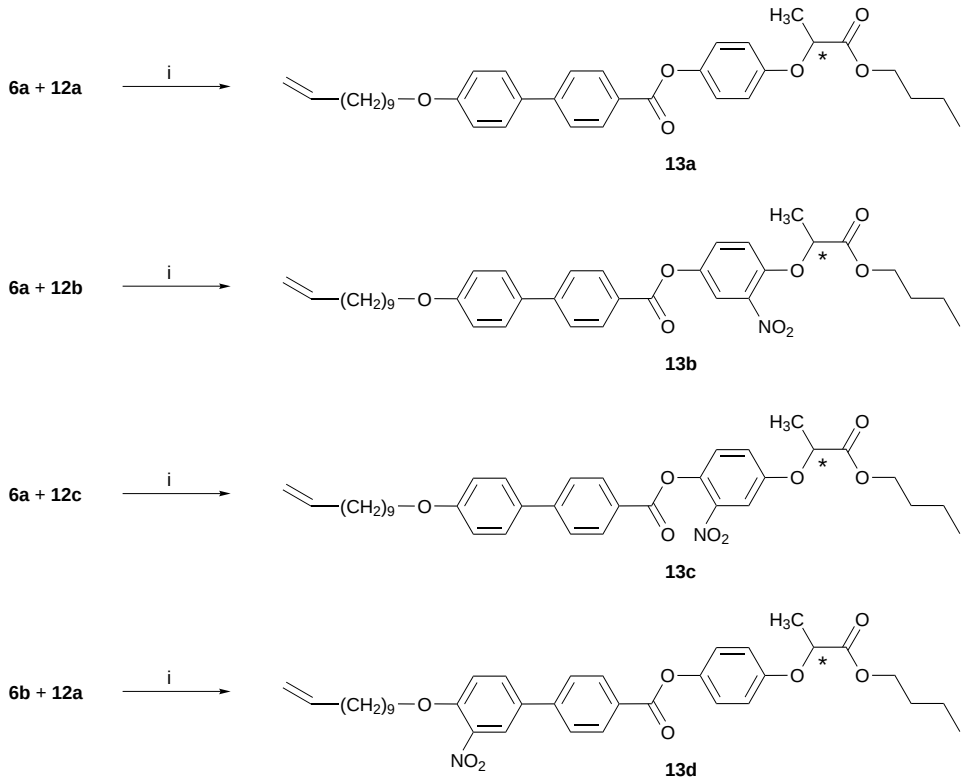

Scheme 3 *Reagents*: i, DCC, DMAP, CH_2Cl_2

7.25 (d, 1 H), 7.81 (d, 2 H), 7.95 (dd, 1 H), 8.00 (d, 2 H), 8.22 (d, 1 H), 11.3 (s, 1 H).

4′-(Undec-10-enyloxy)biphenyl-4-carboxylic acid 6a. The hydroxy-acid **5a** (0.090 mol, 19.3 g) was dissolved in hot ethanol (1500 ml) and water (75 ml) together with potassium hydroxide 86% (11.5 g) and a few crystals of potassium iodide. Undec-10-enyl bromide (0.18 mol) was added and the mixture was refluxed for 24 h. To hydrolyse any ester formed a 10% solution of potassium hydroxide in 70% ethanol was added and refluxing was continued for an additional 3 h. The reaction mixture was allowed to cool and was acidified with concentrated hydrochloric acid. The solid formed was recrystallized from acetic acid and ethanol to yield 22.2 g of product (69%). δ_H ([$^2H_6$] DMSO) 1.2–1.5 (m, 12 H), 1.72 (quintet, 2 H), 2.00 (q, 2 H), 4.00 (t, 2 H), 4.96 (m, 2 H), 5.79 (m, 1 H), 7.03 (d, 2 H), 7.67 (d, 2 H), 7.75 (d, 2 H), 7.98 (d, 2 H).

3′-Nitro-4′-(undec-10-enyloxy)biphenyl-4-carboxylic acid 6b. The acid **6b** was synthesized as for **6a** starting from **5b**. δ_H ([$^2H_6$] DMSO) 1.2–1.5 (m, 12 H), 1.73 (quintet, 2 H), 2.00 (q, 2 H), 4.21 (t, 2 H), 4.96 (m, 2 H), 5.78 (m, 1 H), 7.47 (d, 1 H), 7.85 (d, 2 H), 7.98–8.06 (m, 3 H), 8.24 (d, 1 H).

4-Hydroxyphenyl benzoate 7. A mixture of hydroquinone (0.15 mol, 16.5 g) and pyridine (0.15 mol) in dry methylene chloride was stirred at room temp. Nitrogen was bubbled through and benzoyl chloride (0.14 mol, 19.6 g) was added slowly. After 2 h additional stirring the solvent was evaporated. The solid was washed with water to remove unreacted hydroquinone and then treated with diethyl ether to dissolve the product; the diester remained as it is less soluble in diethyl ether. After evaporation of solvent the product was recrystallized from ethanol with increasing amounts of water. Yield 18.0 g (60%). δ_H ([$^2H_6$] DMSO–$CDCl_3$) 6.87 (d, 2 H), 7.00 (d, 2 H), 7.52 (t, 2 H), 7.65 (t, 1 H), 8.16 (d, 2 H), 9.1 (s, 1 H).

3-Nitro-4-hydroxyphenyl benzoate 8. To hydroquinone monobenzoate **7** (0.04 mol, 8.6 g) in 100 ml of acetic acid,

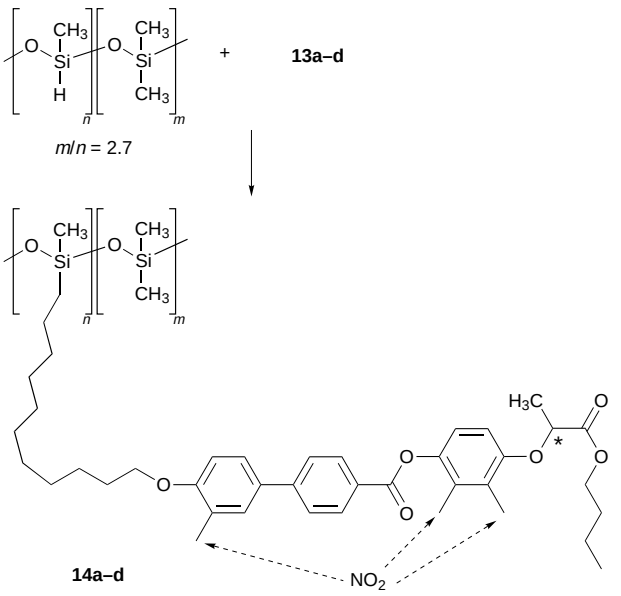

Scheme 4

concentrated nitric acid (11 ml) was added dropwise. The temperature of the reaction mixture was kept below 35 °C. After 50 min the reaction mixture was poured into 700 ml of water. The precipitate was collected and purified on a silica gel column using light petroleum–ethyl acetate (2:1) as eluent. Yield 5.28 g (51%). δ_H ($CDCl_3$) 7.24 (d, 1 H), 7.49 (dd, 1 H), 7.55 (t, 2 H), 7.67 (m, 1 H), 8.01 (d, 1 H), 8.19 (dd, 2 H), 10.5 (s, 1 H).

3-Nitro-4-[(1*R*)-1-ethoxycarbonylethoxy]phenyl benzoate 9 [2-(4-benzoyloxy-2-nitrophenoxy)propanoic acid ethyl ester]. 3-Nitro-4-hydroxyphenyl benzoate **8** (0.016 mol, 4.15 g), *S*-ethyl lactate (0.016 mol, 1.89 g) and triphenylphosphine (0.020 mol) were placed in dry glass equipment with dry THF (100 ml) as

solvent. N_2 gas was bubbled through the mixture at room temp. and diethyl azodicarboxylate (0.020 mol) was added during 30 min. After 3 h of additional stirring at room temp. the solvent was evaporated from the reaction mixture. The resulting solid was dissolved in ethyl acetate and on adding four times the volume of light petroleum, triphenylphosphine oxide was precipitated. The solution was evaporated to dryness and the product recrystallized from light petroleum, 4.76 g (83%). δ_H ($CDCl_3$) 1.26 (t, 3 H), 1.71 (d, 3 H), 4.23 (m, 2 H), 4.84 (q, 1 H), 7.05 (d, 1 H), 7.40 (dd, 1 H), 7.53 (t, 2 H), 7.67 (t, 1 H), 7.79 (d, 1 H), 8.18 (d, 2 H).

2-(2*R*)-(4-Hydroxy-2-nitrophenoxy)propanoic acid 10. To 0.008 mol (2.87 g) of **9** in ethanol (120 ml), 0.016 mol of potassium hydroxide in a few millilitres of water was added. The mixture was stirred overnight at room temp. Ethanol was evaporated and the product was extracted from methylene chloride with water. Water was evaporated and the solid was dissolved in ethyl acetate. The insoluble part was filtered off and the filtrate was evaporated to dryness and used without further purification. δ_H ([$^2H_6$] DMSO) 1.47 (d, 3 H), 4.89 (q, 1 H), 7.01 (dd, 1 H), 7.07 (d, 1 H), 7.19 (d, 1 H), 9.9 (s, 1 H).

2-(2*R*)-(4-Hydroxy-3-nitrophenoxy)propanoic acid 11. To a solution of 2-(2*R*)-(4-hydroxyphenoxy)propanoic acid (0.027 mol, 5.0 g) in acetic acid (100 ml) concentrated nitric acid (1.5 ml) was added dropwise. The temperature of the reaction mixture was kept below 35 °C. After 30 min the reaction mixture was poured into water. The product was extracted from the aqueous phase using diethyl ether. No further purification was done. Yield 5.1 g (80%). δ_H ([$^2H_6$] DMSO) 1.53 (d, 3 H), 4.89 (q, 1 H), 7.11 (d, 1 H), 7.24 (dd, 1 H), 7.39 (d, 1 H), 10.6 (s, 1 H).

Butyl 2-(2*R*)-(4-hydroxyphenoxy)propanoate 12a. A solution of 2-(2*R*)-(4-hydroxyphenoxy)propanoic acid (0.01 mol, 1.9 g) in butanol (150 ml) was treated with hydrogen chloride gas until no further heat was evolved. The reaction mixture was evaporated to dryness. The product was separated by column chromatography on silica gel with light petroleum–ethyl acetate (2:1) as eluent. Yield 1.6 g (64%). $[\alpha]_D^{22}$ + 33.9 ($CHCl_3$). δ_H ($CDCl_3$) 0.88 (t, 3 H), 1.30 (m, 2 H), 1.6 (d + m, 5 H), 4.14 (m, 2 H), 4.65 (q, 1 H), 6.72 (m, 4 H).

Esters **12b** and **c** were synthesized as for **12a** starting from **10** and **11** respectively.

Butyl 2-(2*R*)-(4-hydroxy-2-nitrophenoxy)propanoate 12b. $[\alpha]_D^{22}$ − 84 ($CHCl_3$). δ_H ($CDCl_3$) 0.90 (t, 3 H), 1.31 (m, 2 H), 1.60 (m, 2 H), 1.66 (d, 3 H), 4.16 (m, 2 H), 4.74 (q, 1 H), 6.94 (d, 1 H), 6.97 (dd, 1 H), 7.32 (d, 1 H).

Butyl 2-(2*R*)-(4-hydroxy-3-nitrophenoxy)propanoate 12c. $[\alpha]_D^{22}$ + 77.1 ($CHCl_3$). δ_H ($CDCl_3$) 0.92 (t, 3 H), 1.35 (m, 2 H), 1.64 (d + m, 5 H), 4.18 (m, 2 H), 4.73 (q, 1 H), 7.10 (d, 1 H), 7.27 (dd, 1 H), 7.48 (d, 1 H), 10.3 (s, 1 H).

The last reaction step to the mesogenic side-chain precursors **13a–d** was similar for all and is described for **13b**.

4-[(1*R*)-Butoxycarbonylethoxy]phenyl 4′-(undec-10-enyloxy)biphenyl-4-carboxylate 13a. From **6a** and **12a** as for **13b**. $[\alpha]_D^{22}$ + 18.0 ($CHCl_3$). δ_H ($CDCl_3$) 0.90 (t, 3 H), 1.2–1.5 (m, 14 H), 1.6 (d + m, 5 H), 1.81 (quintet, 2 H), 2.04 (q, 2 H), 4.00 (t, 2 H), 4.17 (m, 2 H), 4.74 (q, 1 H), 4.97 (m, 2 H), 5.81 (m, 1 H), 6.92 (d, 2 H), 7.00 (d, 2 H), 7.13 (d, 2 H), 7.58 (d, 2 H), 7.68 (d, 2 H), 8.21 (d, 2 H).

4-[(1*R*)-Butoxycarbonylethoxy]-3-nitrophenyl 4′-(undec-10-enyloxy)biphenyl-4-carboxylate 13b. From **6a** and **12b**. Dry glassware was used. A mixture of 2 mmol (0.73 g) of **12b**, 2 mmol (0.57 g) of **6a** and 15 mg of dimethylaminopyridine (DMAP) in dry methylene chloride was treated with 4 mmol (0.83 g) of dicyclohexylcarbodiimide (DCC) at 0 °C. The temperature was allowed to rise to room temp. and stirring was continued for 3 h. Urea was filtered off and the filtrate was evaporated to dryness. Column chromatography on silica gel with light petroleum–ethyl acetate (9:1) as eluent gave 1.0 g of pure product (80%). $[\alpha]_D^{22}$ − 28.7 ($CHCl_3$). δ_H ($CDCl_3$) 0.89 (t, 3 H), 1.2–1.5 (m, 14 H), 1.6 (m, 2H), 1.69 (d, 3 H), 1.80 (quintet, 2 H), 2.02 (q, 2 H), 4.00 (t, 2 H), 4.15 (m, 2 H), 4.82 (q, 1 H), 4.95 (m, 2 H), 5.80 (m, 1 H), 6.98 (d, 2 H), 7.03 (d, 1 H), 7.38 (dd, 1 H), 7.58 (d, 2 H), 7.68 (d, 2 H), 7.78 (d, 1 H), 8.18 (d, 2 H).

4-[(1*R*)-1-Butoxycarbonylethoxy]-2-nitrophenyl 4′-(undec-10-enyloxy)biphenyl-4-carboxylate 13c. From **6a** and **12c** as for **13b**. $[\alpha]_D^{22}$ + 21.7 ($CHCl_3$). δ_H ($CDCl_3$) 0.93 (t, 3 H), 1.24–1.43 (m, 12 H), 1.48 (m, 2 H), 1.64 (m, 2 H), 1.69 (d, 3 H), 1.82 (quintet, 2 H), 2.05 (q, 2 H), 4.02 (t, 2 H), 4.21 (t, 2 H), 4.82 (q, 1 H), 4.97 (m, 2 H), 5.82 (m, 1 H), 7.01 (d, 2 H), 7.23 (dd, 1 H), 7.30 (d, 1 H), 7.6 (d + d, 3 H), 7.70 (d, 2 H), 8.22 (d, 2 H).

4-[(1*R*)-Butoxycarbonylethoxy]phenyl-3′-nitro-4′-(undec-10-enyloxy)biphenyl-4-carboxylate 13d. From **6b** and **12a** as for **13b**. $[\alpha]_D^{22}$ + 16.0 ($CHCl_3$). δ_H ($CDCl_3$) 0.92 (t, 3 H), 1.2–1.55 (m, 16 H), 1.64 (d, 3 H), 1.88 (quintet, 2 H), 2.05 (q, 2 H), 4.17 (m, 4 H), 4.75 (q, 1 H), 4.97 (m, 2 H), 5.82 (m, 1 H), 6.94 (d, 2 H), 7.14 (d, 2 H), 7.18 (d, 1 H), 7.69 (d, 2 H), 7.80 (dd, 1 H), 8.13 (d, 1 H), 8.26 (d, 2 H).

Polymers 14a–d. Dry equipment was used. 0.26 g of poly(dimethyl-co-methylhydrogen)siloxane (2.7:1) (corresponding to 1.0 mmol Si-H) and 1.1 mmol of **13a-d** were dissolved in dry toluene (2 ml). Catalyst solution [0.8 ml; dicyclopentadienylplatinum(II) chloride in dry toluene; 0.1 mg ml^{-1}] was added and the reaction flask was sealed with a septum and heated to 110 °C. After 2 d an additional 0.8 ml of catalyst solution was added and heating was continued. The reaction was monitored by IR spectroscopy and further addition of catalyst continued until the Si—H signal at *ca.* 2155 cm^{-1} was constant relative to the C=O signal at *ca.* 1740 cm^{-1}. The reaction mixture was added dropwise to methanol (400–800 ml) during vigorous stirring. The product was collected by centrifugation. Reprecipitation from chloroform in methanol was continued until no free side-chain could be detected by thin layer chromatography. Treatment of the product by dissolving it in ethyl acetate and passing the solution through a 0.2 μm Teflon filter often reduced the amount of remaining Si—H drastically. Yield 0.5–0.8 g. ^1H NMR spectra of the polymers show broader signals than those of the side chain precursors, but are otherwise very similar except that the signals from methyl groups attached to silicon at δ 0–0.16 and a methylene group attached to silicon at δ 0.5 are present, while the olefinic protons at δ 4.95–4.97 and δ 5.80–5.82 are absent. A Si—H signal appeared at δ 4.7, equivalent to 10–15% unreacted hydrogens.

14a $[\alpha]_D^{22}$ + 13.8 ($CHCl_3$).

14b $[\alpha]_D^{22}$ − 10.0 ($CHCl_3$).

14c $[\alpha]_D^{22}$ + 15.3 ($CHCl_3$).

14d $[\alpha]_D^{22}$ + 10.0 ($CHCl_3$).

Sample preparation and electric measurements

For the study of physical properties such as electro-optic effects in smectic liquid crystals, the achievement of well aligned samples is essential. Our standard shear cell,[30] built for measurements on low molar mass ferroelectric liquid crystals, has proved very useful for obtaining aligned polymer samples and was used for all polymeric liquid crystals and some low

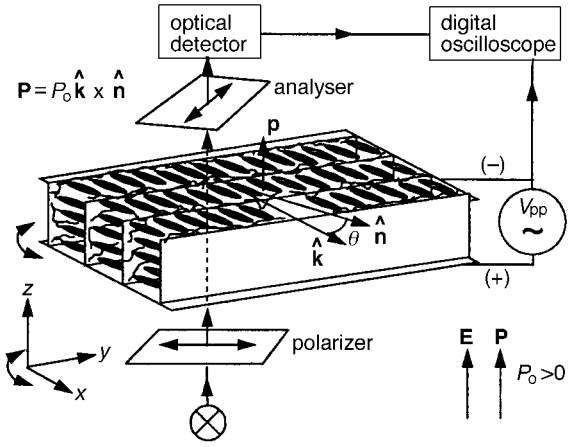

Fig. 1 Experimental set-up and cell geometry

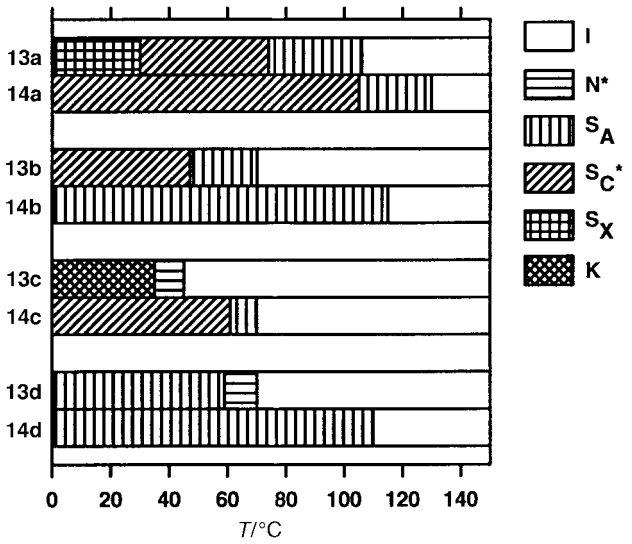

Fig. 2 Phase behaviour of side-chain precursors and polymers

molar mass liquid crystal compounds in this study. The sample is applied to the lower glass plate and melted into the isotropic phase to cover the whole glass area. Then the upper glass plate is put on and the shear cell is assembled. Orientational shear was applied in the smectic A phase close to the isotropic phase. A special electrode pattern ensures that the active area is always 16.8 mm^2, independent of shear position. Spacers consist of thermally evaporated 2 μm SiO_2, and the orientation of the smectic layers is such that the layer normal ($\hat{\mathbf{k}}$) is perpendicular to the shear direction, *cf.* Fig. 1. A 1000 Å protective SiO_2 layer covers the ITO electrodes. The shear alignment cell is mounted in a Mettler FP52 hot stage for temperature control and put in a Zeiss Photomicroscope equipped with a fast electro-optic recording system. The sample temperature is independently measured by a Pt 100 resistor element placed in the sample holder close to the sample. For some of the low molar mass samples good alignment could also be achieved in standard commercial surface-coated cells with 4×4 mm active area and 4 μm thickness, obtained from EHC.

The measurement of the spontaneous polarization P_s was done with either the bridge method or the triangular wave method. The measured polarization is taken from a series of hysteresis curves, where the reading of the amplitude of the loop directly gives the spontaneous polarization by eqn. (1),

$$P_s = \frac{1}{2A}\frac{k\Delta U}{G}C_1 \qquad (1)$$

where A is the active sample area, k is a correction factor for the SiO_2 protective layer ($k = 1.1$ for the shear cell glasses), G is the gain of the instrumental amplifier, ΔU is the amplitude of the loop and C_1 is the reference capacitor in series with the ferroelectric LC sample. In order to measure the smectic tilt angle Θ in the C* phase, we applied a low frequency square wave field and determined the two extinction orientations by rotating the sample between crossed polarizers. To investigate the electroclinic effect, measurements of induced tilt angle and optical response time were carried out as a function of applied field and temperature.

Results and Discussion

Synthesis

The synthetic route to these side chain liquid crystalline polymers consists of four parts as already shown in Schemes 1–4. The synthesis of 4′-hydroxybiphenyl-4-carboxylic acid[9,29] and its etherification also including the 3′-nitro derivatives were straightforward (see Scheme 1). Scheme 2 shows the route to the chiral groups of which two were made from (+)-2-(4-hydroxyphenoxy)propionic acid kindly supplied by BASF. The third chiral group (compound **12b**) was synthesized *via* a Mitsunobu reaction of (*S*)-ethyl lactate with nitrohydroquinone monobenzoate. The reaction was performed under standard Mitsunobu conditions and proceeds with inversion of configuration.[31] In the final step of the side chain precursor synthesis, the biphenylcarboxylic acids were esterified with the chiral propanoic ester derivatives using dicyclohexylcarbodiimide (Scheme 3). The side chain liquid crystalline polymers were finally obtained by a hydrosilylation reaction (Scheme 4). The extent of reaction was monitored by FT-IR. Attempts to quantify the optical purity of the mesogens by ^{1}H NMR using a chiral shift reagent, (+)-praseodymium tris(3-heptafluorobutyrylcamphorate), have been made. Addition of the chiral shift reagent caused no observable separation of peaks, although this has been reported by others.[32] Materials up to three years old show no reduction in the specific optical rotations due to racemization.

Liquid crystal properties

The system used as reference[24] (**13a**, **14a**) is easy to handle during physical measurements and shows typical ferroelectric behaviour. The introduction of a strong electron attracting group at different aromatic positions in the mesogenic core was thought to give indications of the importance of electric dipoles in the mesogen. The influence on spontaneous polarization in the chiral smectic C phase was of special interest.

Phase behaviour. The nitro substituent affected the phase behaviour markedly for the low molar mass materials as can be seen in Table 1 and Fig. 2. The lateral substituent lowers the clearing temperature in all cases, a well-known effect. Furthermore the nitro group alters the type of liquid crystalline phase that appears, depending on substituent position. Only in mesogen **13b** is the smectic C* phase retained and a comparison of ferroelectric behaviour can be made with the reference system, **13a**. In mesogen **13c** the smectic phases are lost and only in a narrow temperature interval does a chiral nematic phase remain. The nitro group *ortho* to the central ester linkage probably induces greater order and thereby causes crystallization. This can be explained by an increase in attractive forces by dipole–dipole interactions between mesogens or by a decrease in intramolecular mobility on introduction of the nitro group in this position. The observed drastic lowering of the clearing temperature would at first make the former explanation less probable but dipole–dipole interactions are known to be strongly temperature dependent[33] and rotation

about the molecular long axis could be restricted by steric or electronic interactions involving the nitro group or by an increased moment of inertia. The location of the substituent towards the centre of the mesogenic core hinders the formation of layered phases. With a different chiral group Walba[22] described similar behaviour although the smectic phases were not completely lost. With the nitro group in the biphenyl as in **13d** a broad smectic A phase and a narrow nematic region are observed (Fig. 2). Compared to **13a** the core is broadened by the nitro substituent which according to Goodby disfavours formation of a smectic C phase.[34] It also reduces the anisotropy of molecular polarizability and increases the polarizability perpendicular to the long molecular axis. This is known to diminish liquid crystalline order,[6] as is also seen in system **13d**.

The changes in phase behaviour when the side-chain precursors are attached to the polysiloxane backbone follows the general expectations. All clearing temperatures are raised by 25–45 °C and crystallization is prohibited (Fig. 2). The stability of the smectic phases is increased at the expense of the nematic phases which disappears. In the polysiloxane systems, microphase separation of main chain and side chains exerts an extra driving force for this formation of layered structures. In the case of **13b** the smectic C* phase cannot be detected when going to polymer **14b** which is somewhat unexpected. Naciri *et al.*[26] reported a smectic C* phase ranging from T_g to 37 °C for a polymer similar to **14b** with one methylene unit less in the spacer and a different co-polymerization ratio in the siloxane backbone. It is possible that polymer **14b** possesses a smectic C* phase but that it has a very short helical pitch which we have not succeeded in unwinding. Therefore the sample behaves as a smectic A phase. Comparing polymer **14a** without a lateral substituent in the mesogenic core with **14b–d** containing a nitro group, it can be seen that the clearing temperatures are lowered by the substituent effect. In **14b** and **14d** the isotropic transition is moved by 15 and 20 °C, respectively. In **14c** the substituent in the central part of the core gives a more drastic effect and the lowering of the transition temperature is 60 °C. Another striking difference is that **14b** and **14d** only exhibit very broad smectic A phases while **14c** has a broad smectic C* phase as well as a smectic A phase. In order to rationalize this let us consider the layer structures of the polymers in relation to the low molar mass mesogens. In most cases of smectic phases of low molar mass mesogens, the layer structure is not especially well defined. This is seen in X-ray studies which then only give the first order reflection. The mesogens are thus able to make use of the most favourable intermesogenic interactions regardless of how much the mesogens overlap each other. In a polymer liquid crystal with smectic phases there is a much more distinct layer structure. This is evident from X-ray diffraction studies where many polymeric smectic A phases show more than one order of reflection.[35] In a polysiloxane system the backbone is confined to sublayers between the liquid crystalline layers because of the microphase separation. This reduces the freedom of mesogen arrangement. The intermesogenic interactions that were favourable in the low molar mass smectic phase may not give the lowest energy arrangement anymore. This can be the case in **14b** and **14d**

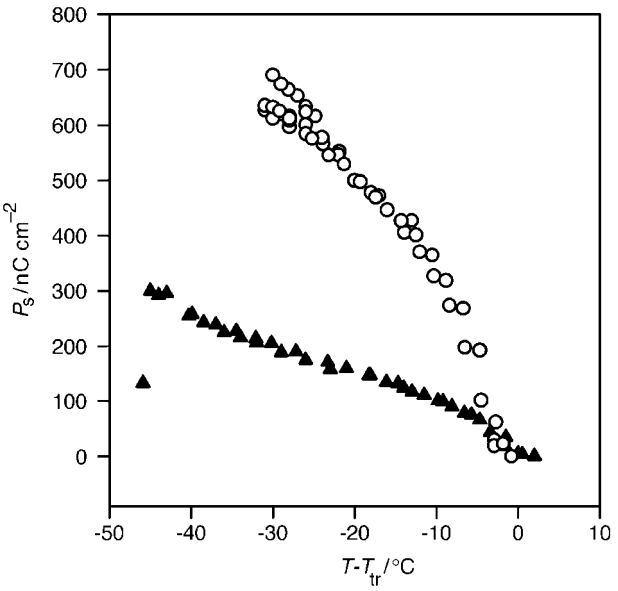

Fig. 3 Spontaneous polarization of side-chain precursors *versus* temperature with reference to S_A–S_C* phase transition: (▲) **13a** and (○) **13b**

which have the polar lateral substituents at the end of the stiff core. The formation of distinct smectic layers is more favourable than polar interactions between mesogens giving a small overlap of the stiff cores. The intermesogenic interactions are reduced and a nitro substituent at the end of the core in the polymeric liquid crystals would favour a smectic A phase over a smectic C*. In the case of **14c** the formation of distinct smectic layers arranges the mesogens to give large overlap of the stiff cores although a disturbing substituent is positioned in the central part of the core. Without the restricting polymer sublayers this substituent causes a longitudinal shift of the mesogens to give only a nematic phase, **13c**. Liquid crystalline phase behaviour seems to depend on a very delicate balance between attractive and repulsive intermesogenic forces. The distance between the mesogens, which is a key parameter, is affected by geometry, electron distribution and polarizability of the mesogen. All these factors change when substituents are introduced or varied and this of course complicates the understanding of lateral substituent effects in liquid crystals.

Electro-optical properties, SmC* phase. The desired evaluation of the influence on ferroelectric behaviour exerted by the nitro group in the mesogenic core becomes rather limited since the smectic C* phase is present only in **13b** and **14c** of the nitro-containing systems. Nevertheless interesting observations can be made. In Fig. 3 the spontaneous polarizations (P_s) of **13a** and **13b** are shown and one particularly interesting effect of the nitro substituent can be seen. To our knowledge a P_s value of *ca.* 700 nC cm^{-2} is the highest reported for a system with one chiral centre. One possible explanation could be the increased double bond character of the phenyl ether bond caused by the nitro group in an *ortho* position. This restricts rotational mobility around the ether linkage.

Table 1 Phases and transition temperatures

material	phase sequence/°C											
13a	S_X		30		S_C*		74		S_A		106	I
13b		−5		S_C*		52		S_A		70		I
13c			K		35		N*		45		I	
13d		−5		S_A		59		N*		70		I
14a		−5		S_C*		105		S_A		130		I
14b				0		S_A		115		I		
14c		0		S_C*		61		S_A		70		I
14d				−10		S_A		110		I		

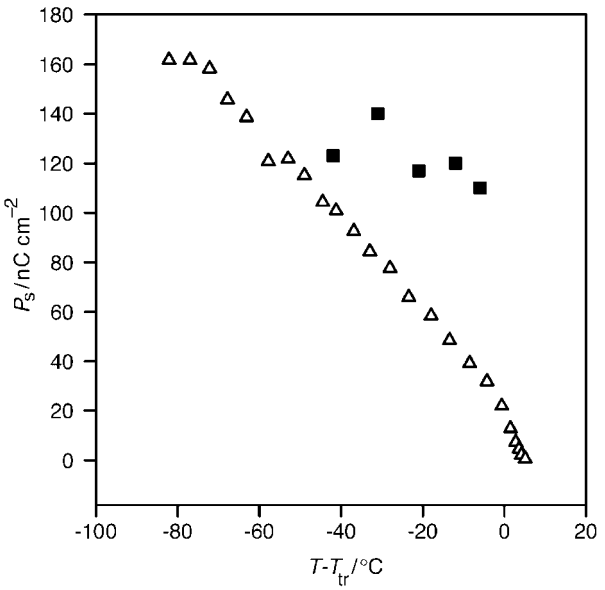

Fig. 4 Spontaneous polarization of polymers *versus* temperature with reference to S_A–S_C* phase transition: (△) **14a** and (■) **14c**

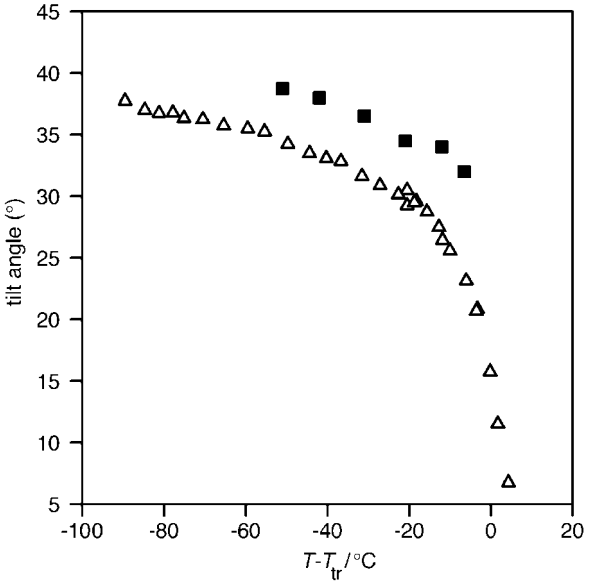

Fig. 6 Tilt angle of polymers *versus* temperature with reference to S_A–S_C* phase transition: (△) **14a** and (■) **14c**

In Fig. 4 the spontaneous polarization of the polymers are presented and **14c** shows values up to twice as high as for **14a** at the same reduced temperatures. Measured tilt angles are a few degrees higher for the nitro containing systems as presented in Fig. 5 and 6. When comparing spontaneous polarization and tilt angle for a system, they usually exhibit the same temperature behaviour, but as is seen in the figures this does not apply for **13a** and **14a**. The analysis of **13c** and **14c** was limited by the easily hydrolysed central ester linkage in the mesogen.

Optical response times (τ_r) are also of interest since they relate to collective side-chain dynamics, and from Fig. 7 and 8 it is clear that for **13b** and **14c** with a nitro substituent in the mesogen, τ_r have a stronger temperature dependence than **13a** and **14a**, respectively. **13b** with a very high P_s has response times in the 100 μs region while **13a** is ten times faster. It is evident that the stronger mesogenic interactions in **13b,** which are responsible for the high spontaneous polarization, are slowing the reorientation of the side-chains. The polymers are slower and show τ_r in the millisecond range but near the smectic A transition polymer **14c** speeds up and response times as low as 10 μs are recorded. The greater temperature dependence of dipole–dipole interactions is a possible explanation for these latter observations.

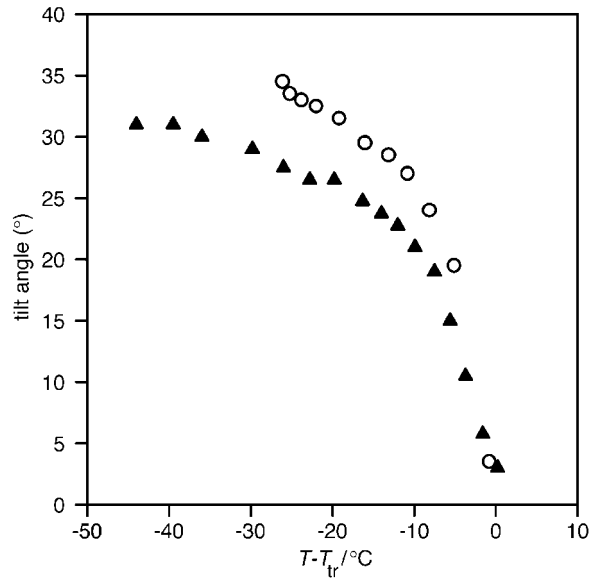

Fig. 5 Tilt angle of side-chain precursors *versus* temperature with reference to S_A–S_C* phase transition: (▲) **13a** and (○) **13b**

Electro-optical properties, SmA phase. Some details of the electro-optical behaviour in the smectic A phase have been examined for the side-chain precursors **13a**, **b**, **d**. In Fig. 9 the temperature dependence of the induced tilt shows the usual steep increase close to the S_A–S_C* transition for **13a** and **b**, while **13d** has a smaller temperature dependence because of the different phase sequence. The variations in induced tilt with applied field are shown in Fig. 10 at 15 °C below the Iso–S_A transition temperature. Linear dependencies were obtained for all three systems.

The induced tilt as a function of temperature for the polymers (Fig. 11) does not give the usual behaviour for **14d**. The curve can be divided into three parts with different slopes. As the

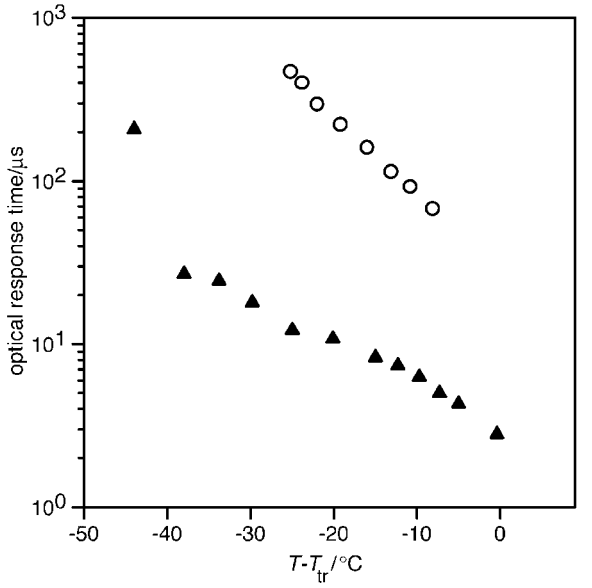

Fig. 7 Response times in the smectic C* phase of side-chain precursors *versus* temperature with reference to S_A–S_C* phase transition, at a field of 8 V μm^{-1}. For comparison the measured values of **13b** were recalculated to this field ($\tau_r \propto 1/E$). (▲) **13a** and (○) **13b**

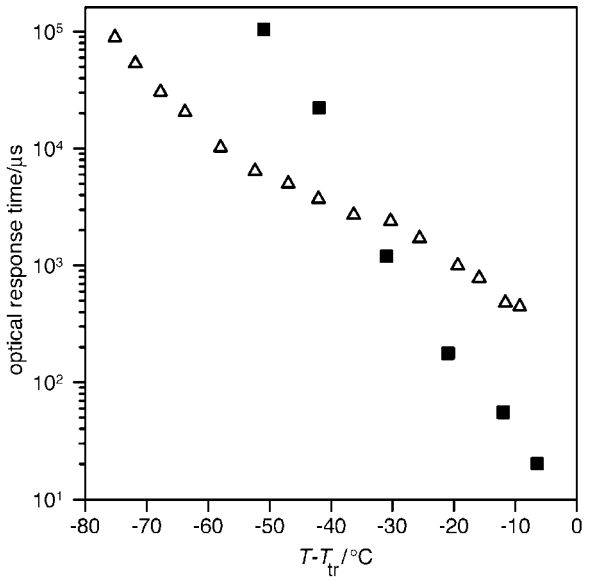

Fig. 8 Response times in the smectic C* phase of polymers *versus* temperature with reference to S_A–S_C* phase transition, at a field of 8 V μm^{-1}. For comparison the measured values of **14c** were recalculated to this field ($\tau_r \propto 1/E$). (△) **14a** and (■) **14c**.

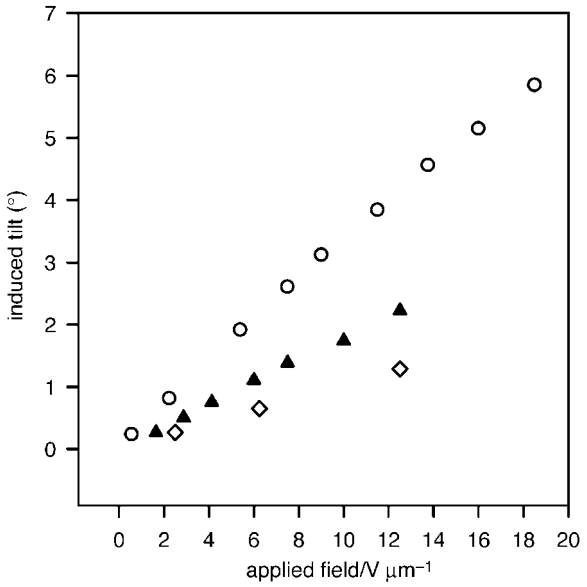

Fig. 10 Induced tilt as a function of applied field for side-chain precursors at 15 °C below the I–S_A phase transition ($T - T_{tr} = -15$ °C): (▲) **13a**, (○) **13b** and (◇) **13d**

phenomenon remains in a plot of the response time as a function of inverse temperature (Fig. 12) it cannot be regarded as a viscosity effect, if the viscosity is assumed to follow an Arrhenius type of behaviour. Are there changes in the mesogenic interactions through the temperature span of the smectic A phase? In Fig. 13 polymers **14b** and **d** show large electroclinic coefficients at low temperatures. This could indicate a smectic C* phase at lower temperatures, but this has not been confirmed. Further investigations of the polymers show response times independent of applied field (Fig. 14). At the same reduced temperatures the response times were within the same order of magnitude for polymers **14a, b** and **d**. When comparing **14b** and **14d** at low temperatures (Fig. 13 and 14), polymer **14b** shows larger electroclinic coefficient and faster response. As the phase sequences are identical these observations can be explained by the difference in position of the nitro group which may cause a larger transverse dipole moment in **14b** compared to **14d**.

Other interesting properties. The side-chain precursor **13b** with its very large spontaneous polarization was of course of interest for NLO measurements. The results from these investigations have been reported earlier.[27] From the SHG-intensity in the smectic C* phase, a d_{eff} value of 0.055 pm V^{-1} was estimated. Furthermore, for the first time a field-controllable SHG-intensity in the smectic A* phase dependent on the square of the applied electric field was reported.

Conclusions

We have studied the effect of introducing nitro substituents in the mesogenic core, and have found it to be considerable. Drastic changes in phase behaviour with substituent position are observed. In one position the nitro group reduces the transition temperatures for the low molar mass compound and more than doubles the maximum spontaneous polarization to a value of *ca.* 700 nC cm^{-2}. Moving the nitro substituent one position in the aromatic ring gives a mesogen

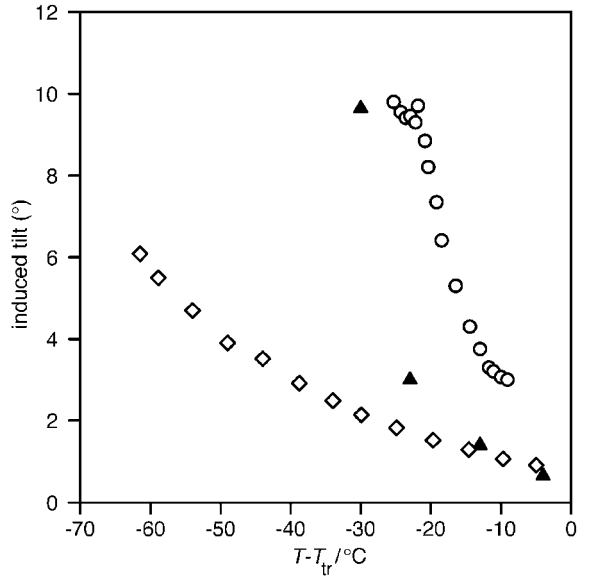

Fig. 9 Induced tilt as a function of temperature with reference to I–S_A phase transition, for side-chain precursors. Applied field 7.5, 16.5 and 12.5 V μm^{-1} for (▲) **13a**, (○) **13b** and (◇) **13d**, respectively.

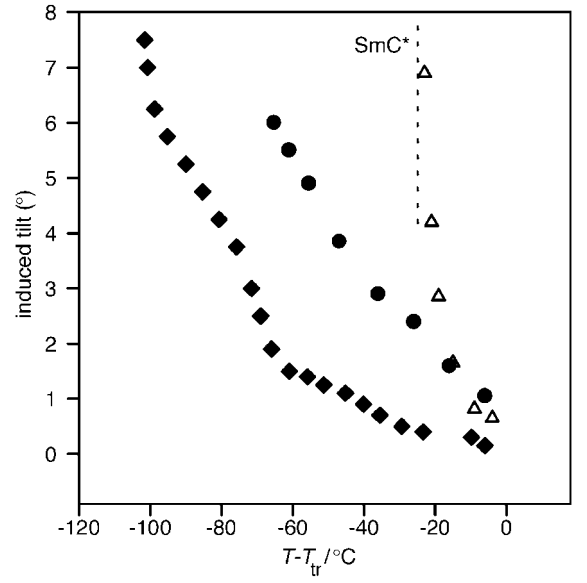

Fig. 11 Induced tilt as a function of temperature with reference to I–S_A phase transition, for polymers. Applied field 16.2, 53.5 and 23.8 V μm^{-1} for (△) **14a**, (●) **14b** and (◆) **14d**, respectively.

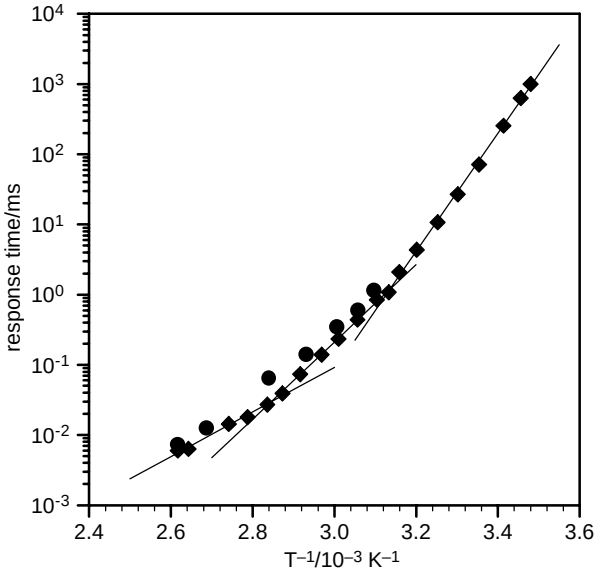

Fig. 12 Response times as a function of inverse temperature. Applied field 53.5 and 23.8 V μm^{-1} for (●) **14b** and (◆) **14d** respectively. The lines are linear regressions of the different parts of the **14d** plot.

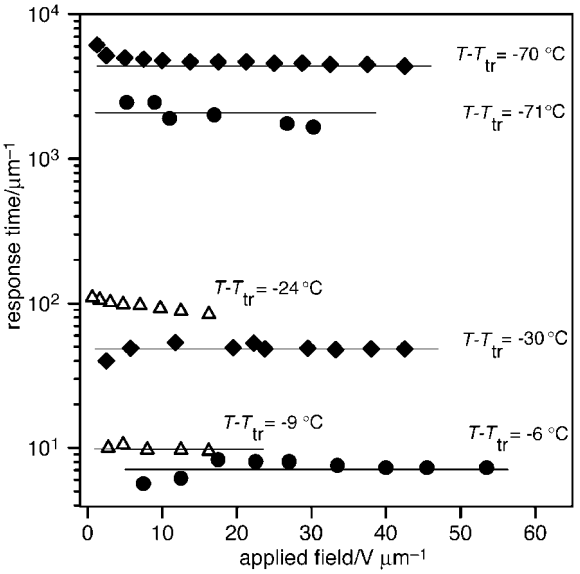

Fig. 14 Response times in the smectic A phase of polymers: (△) **14a**, (●) **14b** and (◆) **14d**. T_{tr} refers to the I–S_A transition. The lines are only a guide to the eye.

with no smectic phases. The position of the lateral nitro substituent has a more pronounced effect in the low molar mass compounds than in the polymer liquid crystals. In the polymers the phase separation of the polymer backbone is a driving force for smectic layer formation and this reduces the effect of the substituents.

The presence of a nitro substituent results in larger tilt angles and stronger temperature dependence of the response time in the smectic C* phase. The comparison of the investigated properties in the smectic A phase is complicated by the differences in phase sequence of the systems caused by the nitro substituents. The nitro group introduces both steric and electronic effects. Apart from changing the geometry of the mesogen it also changes the dipole moment and the polarizability of the mesogen. Depending on substituent position the total effect on phase behaviour and electro-optical properties varies over a considerable range.

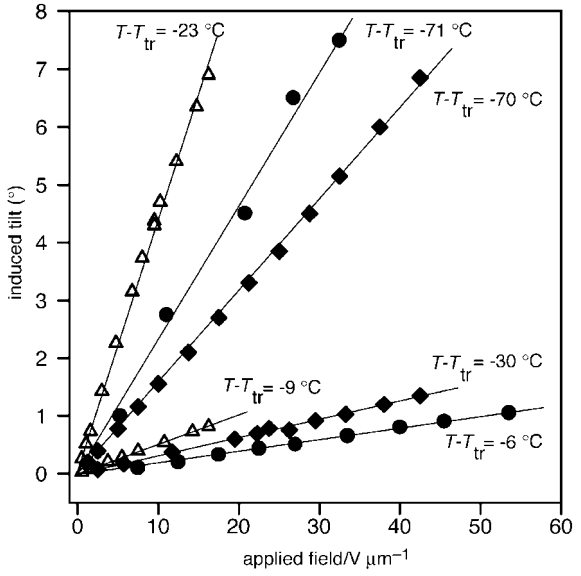

Fig. 13 Induced tilt as a function of applied field for polymers: (△) **14a**, (●) **14b** and (◆) **14d**. T_{tr} refers to the I–S_A transition. The lines are only a guide to the eye.

Financial support from The Swedish Natural Science Research Council, The Swedish Research Council for Engineering Sciences and The Swedish Defence Research is gratefully acknowledged.

References

1 V. P. Shibayev and S. V. Byelyayev, *Polym. Sci. USSR*, 1990, **32**(12), 2384.
2 P. Le Barny and J. C. Dubois, in *Side Chain Liquid Crystal Polymers*, ed. C. B. McArdle, Blackie, Glasgow, and Chapman and Hall, New York, 1989, p. 130.
3 V. P. Shibaev, M. V. Kozlovsky, L. A. Beresnev, L. M. Blinov and N. A. Platé, *Polym. Bull.*, 1984, **12**, 299.
4 N. Shiratori, A. Yoshizawa, I. Nishiyama, M. Fukumasa, A. Yokoyama, T. Hirai and M. Yamane, *Mol. Cryst. Liq. Cryst.*, 1991, **199**, 129.
5 J. W. Goodby and I. Nishiyama, *J. Mater. Chem.*, 1993, **3**(2), 149.
6 G. W. Gray, in *Adv. Liquid Crystals*, ed. G. H. Brown, Academic Press, New York, 1976, p. 1.
7 E. M. Averyanov, *Liq. Crystals*, 1987, **2**(4), 491.
8 G. W. Gray, J. S. Hill and D. Lacey, *Makromol. Chem.*, 1990, **191**, 2227.
9 G. W. Gray, J. B. Hartley and B. Jones, *J. Chem. Soc.*, 1955, 1412.
10 T. Inukai, S. Saitoh, H. Inoue, K. Miyazawa, K. Terashima and K. Furukawa, *Mol. Cryst. Liq. Cryst.*, 1986, **141**, 251.
11 M. Svensson, B. Helgee, K. Skarp, G. Andersson and D. Hermann, *Ferroelectrics*, 1996, **181**, 319.
12 N. F. Cooray, M.-a. Kakimoto, Y. Imai and Y.-i. Suzuki, *Polym. J.*, 1993, **25**, 863.
13 H. Stevens, G. Rehage and H. Finkelmann, *Macromolecules*, 1984, **17**, 851.
14 V. Percec and A. Keller, *Macromolecules*, 1990, **23**, 4347.
15 M. Dumon, H. T. Nguyen, M. Mauzac, C. Destrade, M. F. Achard and H. Gasparoux, *Macromolecules*, 1990, **23**(1), 355.
16 H. Poths, E. Wischerhoff, R. Zentel, A. Schönfeld, G. Henn and F. Kremer, *Liq. Cryst.*, 1995, **18**(5), 811.
17 R. Zentel and H. Poths, *Liq. Cryst.*, 1994, **16**(5), 749.
18 M. A. Osman, *Mol. Cryst. Liq. Cryst.*, 1985, **128**, 45.
19 Y. Masuda, Y. Sakurai, H. Sugiura, S. Miyake, S. Takenaka and S. Kusabayashi, *Liq. Cryst.*, 1991, **10**(5), 623.
20 C. J. Booth, J. W. Goodby, J. P. Hardy, O. C. Lettington and K. J. Toyne, *J. Mater. Chem.*, 1993, **3**(9), 935.
21 M. Hird, K. J. Toyne, P. Hindmarsh, J. C. Jones and V. Minter, *Mol. Cryst. Liq. Cryst.*, 1995, **260**, 227.
22 D. M. Walba, M. B. Ros, N. A. Clark, R. Shao, K. M. Johnson, M. G. Robinson, J. Y. Liu and D. Doroski, *Mol. Cryst. Liq. Cryst.*, 1991, **198**, 51.
23 M. Ozaki, M. Sakuta, K. Yoshino, B. Helgee, M. Svensson and K. Skarp, *Appl. Phys. B*, 1994, **59**, 601.

24 B. Helgee, T. Hjertberg, K. Skarp, G. Andersson and F. Gouda, *Liq. Cryst*., 1995, **18**(6), 871.
25 M. Svensson, B. Helgee and K. Skarp, *Conference paper (presentation)*, in *International conference on liquid crystal polymers*, 1994, Beijing, China.
26 J. Naciri, B. R. Ratna, S. Baral-Tosh, P. Keller and R. Shashidhar, *Macromolecules*, 1995, **28**, 5274.
27 K. Kobayashi, T. Watanabe, S. Uto, M. Ozaki, K. Yoshino, M. Svensson, B. Helgee and K. Skarp, *Jpn. J. Appl. Phys*., 1996, **35**, L104.
28 R. Shashidhar, J. Naciri, G. P. Crawford and B. R. Ratna, *Ferroelectrics*, 1993, **148**, 297.
29 V. Percec, Q. Zheng and M. Lee, *J. Mater. Chem*., 1991, **1**(4), 611.
30 K. Skarp and G. Andersson, *Ferroelectrics Lett*., 1986, **6**, 67.
31 O. Mitsunobu, *Synthesis*, 1981, 1.
32 C. J. Booth, G. W. Gray, K. J. Toyne and J. Hardy, *Mol. Cryst. Liq. Cryst*., 1992, **210** 31.
33 M. A. Osman, *Z. Naturforsch. Teil A*, 1983, **38a**, 693.
34 J. W. Goodby, in *Ferroelectricity and related phenomena*, vol. 7, *Ferroelectric liquid crystals: Principles, properties and applications*, ed. G. W. Taylor, Gordon and Breach, 1991, p. 99.
35 P. Davidson and A. M. Levelut, *Liquid Crystals*, 1992, **11**(4), 469.

Paper 7/04918H; *Received* 11*th July*, 1997